Numerical simulations of black-hole binaries and gravitational wave emission

Ulrich Sperhake[a,b,c,d], Emanuele Berti[b,d], Vitor Cardoso[c,d]

[a]*Institute of Space Sciences (CSIC-IEEC), Campus UAB, Torre C5 parells, 08193 Bellaterra, SPAIN*
[b]*California Institute of Technology, 1200 E California Boulevard, Pasadena, CA 91125, USA*
[c]*CENTRA, Departamento de Física, Instituto Superior Técnico, Universidade Técnica de Lisboa - UTL, Av. Rovisco Pais 1, 1049 Lisboa, Portugal.*
[d]*Department of Physics and Astronomy, The University of Mississippi, University, MS 38677, USA*

Abstract

We review recent progress in numerical relativity simulations of black-hole (BH) spacetimes. Following a brief summary of the methods employed in the modeling, we summarize the key results in three major areas of BH physics: (i) BHs as sources of gravitational waves (GWs), (ii) astrophysical systems involving BHs, and (iii) BHs in high-energy physics. We conclude with a list of the most urgent tasks for numerical relativity in these three areas.

Keywords: Numerical Relativity, Black Holes, Gravitational Wave Physics, Astrophysics, High-Energy Physics
2000 MSC: 65M06, 65M50, 65M70, 65Z05

1. Introduction

For almost a century now after its discovery, the Schwarzschild solution describing a static, spherically symmetric vacuum spacetime in Einstein's theory of general relativity (GR) has been a valuable tool for a wealth of theoretical and experimental studies, including in particular weak-field tests of the theory. For more than half a century, the validity of the solution beyond the Schwarzschild radius $r = 2GM/c^2$ and the consequent existence of BHs was thought to be a mathematical artifact of the field equations. This picture has changed dramatically in more recent decades. Crucial events in

this sense were the mathematical discovery of the Kerr solution describing rotating BHs [1], and the astrophysical X-ray and radio observations in the 1960s and 1970s. Cosmic X-ray sources, first detected in 1963 [2], were soon associated with compact stellar objects and, in particular, with mass exchange from an ordinary star onto a compact object in binary systems [3]. This interpretation received further support when the X-ray source Cyg X-1 was identified with the supergiant BOIb star HD 226868 [4, 5], which established Cyg X-1 as the first observed X-ray binary. Over the next few years, the explanation of these systems in terms of accretion onto compact stellar objects in binary systems became widely accepted (see [6] for a review). Measurements of the binary period and radial velocity provide lower limits on the mass of the compact companion. The values obtained for some X-ray binaries comfortably exceed the upper mass limit of about 3 $M_\odot$ for neutron stars. Recent investigations of Cyg X-1, for example, predict 8.7 ± 0.8 $M_\odot$ for the compact member [7].

Also starting in the early 1960s, optical and radio observations identified "star like" objects with surprisingly large redshifts [8, 9]. If interpreted as cosmological in origin, the redshifts implied enormous distances and, accordingly, luminosities. Over the next decade the cosmological origin of these "quasi-stellar" sources (or quasars) became clear, and accretion onto supermassive BHs (SMBHs) [10, 11] was accepted as the most plausible explanation of their energetics [12, 13]. By now, observations of stellar dynamics near the centers of galaxies and iron Kα emission line profiles provide strong evidence that many galaxies harbor BHs at their centers [14, 15]. BH masses are generally closely correlated to the bulge velocity dispersion and luminosity [16, 17]. For the Milky Way, astrometric and radial velocity observations of short-period stars orbiting the galactic center [18, 19] predict an unseen gravitational mass of $4.1 \pm 0.6 \times 10^6$ $M_\odot$.

Electromagnetic observations provide strong but *indirect* evidence for the existence of astrophysical BHs. A more direct way of probing the BH nature of astrophysical compact objects is offered by the newly emerging field of GW astronomy. First-generation ground-based laser-interferometric detectors (such as LIGO, VIRGO and GEO600) have reached design sensitivity, and advanced versions of these detectors will be operational within a few years [20, 21, 22]. One of the most prominent sources of detectable GWs for these detectors is the inspiral and coalescence of stellar mass and, possibly, intermediate-mass BH (IMBH) binaries. At lower frequencies, space-based laser interferometric observations [23] have the potential to comple-

ment ground-based efforts with high signal-to-noise ratio observations of massive BH binaries. Space-based detectors are guaranteed to observe galactic binaries containing white dwarfs and/or neutron stars, and they may also detect the inspiral of stellar compact objects into massive BHs. Due to the weak interaction of GWs with any type of matter, including the detectors, digging physical signals from the noisy data stream represents a daunting task and heavily relies on so-called *matched filtering* techniques [24]. Matched filtering is a common choice to search for signals of known form in noisy data, and works by cross-correlating the actual "signal" (i.e., the detector's output) with a set of theoretical templates. Accurate modeling of the GW sources thus plays a vital role in maximizing the scientific output from these experimental efforts.

Event rate estimates for IMBHs and stellar-mass BH binaries are very uncertain, but advanced Earth-based detectors are expected to observe several events per year (see [25] for a review). Belczynski *et al.* noted that recent metallicity measurements require revisions in the population synthesis models used for event rate estimates, suggesting that stellar-mass BH-BH binaries may be the first GW sources to be detected [26]. The observations of two possible X-ray binary precursors of BH-BH binaries provide a much needed observational constraint on compact binaries containing at least one BH, suggesting again that BH-BH binary mergers may be more common than anticipated [27]. Population synthesis models have large uncertainties, related e.g. to the poorly known common envelope phase, and some models would necessarily be ruled out if Advanced LIGO does *not* detect BH binaries. In this sense, GW detectors are *guaranteed* to put constraints on compact binary formation in the near future. Schutz [28] also pointed out that coherent data analysis using three or more detectors may further increase event rates by factors of a few, making prospects of doing astrophysics with Earth-based detectors even brighter. Estimates for event rates of SMBH binaries detectable by space-based interferometers range from 0.1 to 1000s per year, with a most likely estimate of $\sim 20 - 30$ [29, 30, 31, 32].

Over the past decade, BH modeling has also attracted a great deal of interest in the context of high-energy physics. According to the gauge/gravity duality, gravitational physics in anti-de Sitter (AdS) backgrounds describes field theories on the boundary of that spacetime [33, 34]. According to this duality, BHs in AdS are dual to an equilibrium field theory, and therefore interacting BHs or BHs off-equilibrium may represent interesting physics from the dual point of view. In fact, there is some evidence that some of

3

the physics behind quark-gluon plasma formation in heavy-ion collisions is captured by this duality, which on the gravitational side corresponds to shock wave collisions and BH formation in AdS [35].

Understanding BH spacetimes is also of interest for high-energy physics in connection with extra-dimensional scenarios. Solutions to the hierarchy problem in physics have been developed where all standard-model interactions are confined to a 3+1 dimensional brane embedded in a spacetime with large extra dimensions or an extra dimension with a warp factor [36, 37]. In these models gravity propagates in the entire higher-dimensional spacetime (the "bulk"), and the fundamental Planck scale could be as low as 1 TeV. These energy scales are accessible to experiments such as the Large Hadron Collider (LHC). If the fundamental Planck scale is so low, Thorne's hoop conjecture suggests the exciting possibility of BH production in high-energy parton-parton collisions [38, 39], i.e. a direct observable signature of the existence of extra-dimensions. Accurate modeling of energy and momentum losses in the form of GWs during the collisions and determination of the BH formation cross section will be crucial for the analysis of data from such experiments (see e.g. [40]), and they should be amenable to classical calculations in D-dimensional GR [41].

Finally, the understanding of BH dynamics under extreme conditions is fascinating from a mathematical-physics point of view. Questions such as BH stability, cosmic censorship, etcetera can only be addressed by solving the full nonlinear set of the field equations.

For many of these scenarios, it is convenient to divide the coalescence of a BH binary in the framework of GR into three stages which mirror the different tools used for their modeling: (i) The inspiral phase, where the interaction between the individual holes is still sufficiently weak to justify the use of post-Newtonian (PN) techniques [42]; (ii) The final orbits, plunge and merger, which are governed by the strong-field regime of Einstein's equations and can be described only by fully numerical simulations; (iii) The ringdown of the remnant BH, which is amenable to a perturbative treatment [43, 44, 45].

In this article we will focus on the second, strong-field stage, on the numerical tools dedicated to its study, and results obtained following the 2005 breakthroughs [46, 47, 48]. As we shall see, however, a comprehensive understanding of BH dynamics requires a close interplay of numerical and analytical studies, and we will discuss in various cases the interface between numerical relativity and approximation techniques.

Following a brief summary of the framework employed in numerical rel-

ativity (Sec. 2), in Secs. 3-5 we will present the main results obtained from numerical studies of BHs in the context of GW detection, astrophysics and high-energy physics, respectively. We conclude in Sec. 6 with a discussion of future applications of numerical relativity. At the end of each section we will provide references to the literature for further reading.

Notation: We shall be using geometrical units, such that the gravitational constant $G = 1$ and the speed of light $c = 1$. We denote spacetime indices $0 \ldots D - 1$ by Greek letters, and spatial indices $1 \ldots D - 1$ by Latin letters.

2. Numerical modeling of black holes

In Einstein's GR, spacetime is modelled as a D-dimensional manifold with a metric $g_{\alpha\beta}$ of Lorentzian signature $- + + + \ldots$. With the exception of Sec. 5 we will restrict our discussion to $D = 4$, i.e. three spatial and one time dimension. The metric is determined by the Einstein equations

$$G_{\alpha\beta} \equiv R_{\alpha\beta} - \frac{1}{2}g_{\alpha\beta}R = T_{\alpha\beta}, \tag{1}$$

with $T_{\alpha\beta} = 0$ in vacuum. While analytic solutions (as, for example, the Schwarzschild and Kerr solutions and the Friedmann-Lemaître-Robertson-Walker solution) have been found for systems with high symmetry, solutions for dynamical configurations without special symmetries generally require the use of numerical tools. For this purpose the Einstein equations need to be cast as an *initial value formulation* such that the Cauchy-Kowalewski theorem guarantees a uniquely determined evolution of appropriately chosen initial data. In the case of Einstein's equations, it is not obvious that such a formulation can be obtained: a straightforward calculation shows that Eq. (1) contains second time derivatives of the metric components g_{ab}, but not of $g_{t\alpha}$. This fact mirrors the coordinate or gauge freedom characteristic of GR, and implies the existence of so-called *constraint* equations which impose conditions on the metric components and their first derivatives on each spatial slice with constant coordinate time t. In the following we will discuss two approaches which provide an initial value formulation of the Einstein equations and have led to successful, long-term stable numerical evolutions: the generalized harmonic (GH) formulation employed in Pretorius' breakthrough BH binary simulations [46] and the canonical Arnowitt-Deser-Misner (ADM) split [49], reformulated by York [50], which forms the starting point for the *moving puncture* breakthroughs [47, 48].

ADM 3+1 Split: Spacetime is decomposed into a one-parameter family of three-dimensional spatial slices. We choose coordinates adapted to this formulation, such that the coordinate time t labels each slice and x^i denotes points on the slice. On each hypersurface, there exists a unique time-like, future pointing unit normal field n^α which defines a projection operator $\perp^\alpha_{\ \beta} = g^\alpha_{\ \beta} + n^\alpha n_\beta$ onto the hypersurface. The geometry of the hypersurface is completely determined by the *three-metric* or *first fundamental form* $\gamma_{ij} \equiv \perp^\mu_{\ i}\perp^\nu_{\ j}g_{\mu\nu} = g_{ij}$. The coordinate freedom is represented by the shift vector $\beta_i \equiv g_{ti}$ and the lapse function $\alpha \equiv \sqrt{g_{tt} - \beta^m\beta_m}$ (with $\beta^i \equiv \gamma^{im}\beta_m$), which relate spatial coordinates on (and measure separation in proper time between) different hypersurfaces. The projections $\perp^\alpha_{\ i}\perp^\beta_{\ j}G_{\alpha\beta}$, $\perp^\alpha_{\ i}G_{\alpha\mu}n^\mu$, $G_{\mu\nu}n^\mu n^\nu$ of the Einstein equations then lead to six evolution equations for the three-metric γ_{ij}, three momentum constraints and the Hamiltonian constraint:

$$\partial_t \gamma_{ij} = \beta^m\partial_m\gamma_{ij} + \gamma_{mi}\partial_j\beta^m + \gamma_{mj}\partial_i\beta^m - 2\alpha K, \tag{2}$$

$$\partial_t K_{ij} = \beta^m\partial_m K_{ij} + K_{mi}\partial_j\beta^m + K_{mj}\partial_i\beta^m - D_i D_j\alpha$$
$$+\alpha\left(\mathcal{R}_{ij} + KK_{ij} - 2K_{im}K^m_{\ j}\right), \tag{3}$$

$$\mathcal{H} \equiv \mathcal{R} + K^2 - K_{mn}K^{kn} = 0, \tag{4}$$

$$\mathcal{M}^i \equiv D_m\left(K^i m - \gamma^{im}K\right) = 0, \tag{5}$$

where $\mathcal{R}_{ij}$, $\mathcal{R}$ and D_i denote the Ricci tensor, Ricci scalar and covariant derivative associated with the three-metric, and the extrinsic curvature K_{ij} has been introduced to obtain a first-order system in time.

It turns out that this formulation of the Einstein equations is only *weakly hyperbolic* [51], and therefore not suitable for long-term stable numerical evolutions. Motivated by these stability problems, several modifications of the ADM system have been investigated. The most popular is the Baumgarte-Shapiro-Shibata-Nakamura (BSSN) formulation [52, 53], which rearranges the degrees of freedom via a split of the extrinsic curvature into trace and trace-free parts, a conformal transformation and promotion of the contracted conformal Christoffel symbols to the status of independent variables:

$$\phi = \frac{1}{12}\ln\gamma, \qquad \tilde{\gamma}_{ij} = e^{-4\phi}\gamma_{ij},$$

$$K = \gamma^{ij}K_{ij}, \qquad \tilde{A}_{ij} = e^{-4\phi}\left(K_{ij} - \frac{1}{3}\gamma_{ij}K\right),$$

$$\tilde{\Gamma}^i = \tilde{\gamma}^{mn}\tilde{\Gamma}^i_{\ mn} = \frac{1}{2}\tilde{\gamma}^{mn}\tilde{\gamma}^{ik}\left(\partial_m\tilde{\gamma}_{nk} + \partial_n\tilde{\gamma}_{km} - \partial_k\tilde{\gamma}_{mn}\right). \tag{6}$$

The resulting set of evolution and constraint equations is given in Eqs. (15)-(30) of [54]. Subject to minor modifications, such as replacing the conformal factor by $\chi \equiv e^{-4\phi}$ or adding the auxiliary constraint arising from the definition of $\tilde{\Gamma}^i$ in Eq. (6), this formulation is employed in the present generation of moving puncture evolution codes [55, 56, 57, 58, 59, 60, 61] which fix the gauge via "1+log" slicing and the Γ-driver condition [54, 62, 63, 64].

GH formulation: Harmonic coordinates are defined by the condition $g_{\alpha\mu}\Box x^\mu = -\Gamma_\alpha = 0$, where $\Box \equiv \nabla^\mu\nabla_\mu$ represents the scalar wave operator. These coordinates have played an important role in the analysis of the Cauchy problem in GR [65, 66, 67]. In harmonic coordinates, the Einstein equations take on a manifestly hyperbolic form, which allows for a generalization to arbitrary coordinate or gauge choices [68, 69]. The first step is to introduce four arbitrary source functions H^α such that the coordinates obey

$$- \Gamma^\alpha = \Box x^\alpha = H^\alpha, \tag{7}$$

and treat these functions as independent evolution variables. Then one considers the GH system

$$R_{\alpha\beta} - \nabla_{(\alpha}C_{\beta)} = 0, \tag{8}$$

where $C_\alpha \equiv H_\alpha + \Gamma_\alpha$. Eq. (8) is equivalent to the Einstein equations, subject to the validity of the constraint (7). In expanded form, the GH system is given by

$$g^{\mu\nu}\partial_\mu\partial_\nu g_{\alpha\beta} = -2\nabla_{(\alpha}H_{\beta)} + 2g^{\mu\nu}g^{\kappa\lambda}\left(\partial_\kappa g_{\mu\alpha}\partial_\lambda g_{\nu\beta} - \Gamma_{\alpha\mu\kappa}\Gamma_{\beta\nu\lambda}\right), \tag{9}$$

and the constraints $C_\alpha = 0$ are preserved by virtue of the Bianchi identities provided that C_α and $\partial_t C_\alpha$ vanish on the initial hypersurface $t = 0$. A key ingredient in the numerical evolution of the GH system is the addition of a constraint damping term $\propto \left[2\delta^\mu_{(\alpha}t_{\beta)} - g_{\alpha\beta}t^\mu\right]C_\mu$ to the right hand side of Eq. (9) [70]. Here, t^μ is a non-vanishing timelike vector field. Finally, it is interesting to note that the Hamiltonian and momentum constraints are automatically satisfied on the initial hypersurface if $C_\alpha = 0 = \partial_t C_\alpha$ [71].

The coordinates were determined in Pretorius' initial simulations by

$$\Box H_t = -\xi_1\frac{\alpha - 1}{\alpha} + \xi_2 n^\nu\partial_\nu H_t, \quad H_i = 0, \tag{10}$$

and the evolution of the metric proceeds according to Eq. (9) with the constraint damping term of Gundlach *et al.* [70]. For further discussion of gauge choices in the GHG system, see also [72, 73].

The spectral code originally developed by the Caltech-Cornell group (see [74, 75] and references therein) employs a first-order version of the GH system [71] with dual-coordinate frames and BH excision. Furthermore, the first-order GH formulation facilitates the specification of constraint-preserving boundary conditions [71]. During the inspiral phase, they evolve the gauge functions H_α such that they remain constant in a frame comoving with the BHs, but switch to a dynamic evolution during the plunge and ringdown; see Sec. III in [76]. While more complex in structure, this framework enables their code to generate BH evolutions with exceptional accuracy [77, 76].

Initial data: The construction of initial data requires solving the Hamiltonian and momentum constraints. Here we only summarize the key concepts; we refer the reader to Cook's review article [78] for details. Most work on the construction of initial data is based on the York-Lichnerowicz split [79, 50], which involves a conformal transformation of metric and extrinsic curvature and separates the latter into trace and trace-free part. More recently, the *thin-sandwich* construction [80], which replaces the extrinsic curvature by the time derivative of the metric, has become a popular alternative. In either case, the resulting elliptic equations simplify substantially under the assumption of conformal flatness and a spatially constant K.

While this formalism provides a convenient method to solve the constraint equations, we still need to ensure that the initial data represent a physically realistic system, typically two BHs with specific spins and momenta. This can be achieved by generalizing the Schwarzschild solution, which is obtained in the above framework in conformally flat form with conformal factor $\exp(\phi) = 1 + \frac{m}{2r}$. A generalization to initial data of N BHs starting from rest is directly obtained by the construction of Misner [81] or Brill and Lindquist [82]. Remarkably, an analytic solution for the extrinsic curvature can still be obtained for BHs with initial linear momenta $\mathbf{P}_n$ and spins $\mathbf{S}_n$ [83]. By applying a compactification to the internal asymptotically flat region, Brandt & Brügmann [84] arrived at the so-called *puncture data* construction, which is the method of choice for most numerical evolutions employing the BSSN formulation. In order to overcome an upper limit of ≈ 0.93 for the dimensionless spin of BHs in puncture type initial data [85], Lovelace *et al.* [86] generated initial data based on a generalization of the Kerr-Schild solution [87] and were thus able to evolve a BH binary with spin magnitude 0.95.

In alternative to generalizing analytically known BH solutions, the pres-

8

ence of horizons in the initial data can be encoded in the form of boundary conditions for the metric and extrinsic curvature [88, 89] as determined by the isolated horizon framework [90]. Initial data along these lines have been constructed in [88, 89], and form the starting point of most of the numerical evolutions using the GH system (see e.g. [91, 75]).

Diagnostics: Extracting physical information from numerical simulations of the Einstein equations is nontrivial for two reasons. First, the evolved variables are dependent on the coordinate conditions; second, it is often not possible to define local quantities familiar from Newtonian physics. The first difficulty requires the calculation of gauge-independent variables. The second difficulty is alleviated by the *isolated horizon* framework [90], which facilitates the calculation of BH mass and spin in the limit of isolated BHs; in practice, this framework is often applied when the BHs are farther apart and their interaction is considered negligible. Local properties of the BHs are encoded in their apparent horizon [93, 94, 95, 96]. In particular, the irreducible mass can be expressed in terms of the apparent horizon area: $M_{\mathrm{irr}} = \sqrt{A_{\mathrm{AH}}/16\pi}$. In the limit of an isolated BH, the spin can be derived from the integration of the rotational Killing vectors over the horizon according to Eq. (8) of [96]. In practice it has been found that using *flat-space* rotational Killing vectors yields reasonable results [97]. It is important to bear in mind, however, the approximate nature of any spin calculation in BH binary simulations.

In comparison, it is more straightforward to extract global quantities of the spacetime, most notably the total mass-energy M_{ADM} and the linear and angular momentum P_i, J_i [49, 50]. These are given by surface integrals at spatial infinity, see e.g. Eqs. (7.15), (7.56) and (7.63) in [92].

Arguably the most important diagnostic quantity in BH simulations is the GW signal. The most common method to extract GWs is based on the Newman-Penrose formalism [98] and derives the complex Newman-Penrose scalar Ψ_4 from contraction of the Weyl tensor with suitably chosen tetrad vectors [99], Sec. III A in [59]. It is often convenient to decompose Ψ_4 into multipoles ψ_{lm} using spherical harmonics of spin-weight -2: $\Psi_4(t, r, \theta, \phi) = \sum_{l=2}^{\infty} {}_{-2}Y_{lm}(\theta, \phi)\psi_{lm}(t, r)$. Contemporary numerical codes typically evaluate Ψ_4 at finite coordinate radius. This results in systematic errors, due to ambiguities in the tetrad choice and the neglect of GW backscattering. While these errors can be reduced by extracting GWs at a sequence of radii and extrapolating to infinite radius (Ψ_4 asymptotically falls off $\sim r^{-1}$ [100]), a cleaner method is to calculate Ψ_4 at infinity as provided by *Cauchy-*

characteristic extraction methods [101, 102, 103]. From Ψ_4, one straight-forwardly obtains the energy, linear and angular momentum radiated in the form of GWs; see e.g. Eqs. (49)-(51) in [59]. In GW data analysis it is more common to work with the wave strain

$$h \equiv h_+ - ih_\times = \int_{-\infty}^t dt' \int_{-\infty}^{t'} dt'' \Psi_4, \qquad (11)$$

decomposed into multipoles: $h(t, r, \theta, \phi) = \sum_{l=2}^\infty {}_{-2}Y_{lm}(\theta, \phi)h_{lm}(t, r)$. In practice, after integrating Ψ_4 twice in time the signal can be severely affected by nonlinear drifts, which can be controlled to a significant extent by performing the integration in the frequency domain [104, 105].

Alternatively, GWs can be extracted by viewing the metric in the far field regime as a perturbation of the Schwarzschild spacetime and employing the formalism of Regge, Wheeler [106] and Zerilli [107, 108]. One thus obtains the Regge-Wheeler-Moncrief and Zerilli-Moncrief master functions $Q_{lm}^\times$, Q_{lm}^+, which can be converted into the multipolar components of the GW strain h according to Eq. (49) of [109].

For a comprehensive summary of the numerical framework for evolving Einstein's field equations, we refer the reader to the books by Alcubierre [51] and Baumgarte and Shapiro [110]. Further details, including mathematical aspects of the equations and characteristic techniques, can be found in the review articles [111, 92, 112].

3. Gravitational wave physics

BH binary systems represent one of the most promising sources of detectable GWs. The parameters of a BH binary are commonly divided into *intrinsic* and *extrinsic* [113]. Intrinsic parameters characterize physical properties of the system, such as the total mass M, the mass ratio $q \equiv M_2/M_1 \leq 1$, the individual BH spins $\mathbf{S}_1$, $\mathbf{S}_2$ and the orbital eccentricity. Extrinsic parameters such as sky position, distance, orbital inclination angle, arrival time and initial phase of the wave, in contrast, depend on the source location relative to the observer, and do not directly enter the GW source modeling process.

The majority of numerical studies of BH binary spacetimes performed to date have focussed on comparable mass-ratios $q \geq 1/10$ and moderate spin magnitudes $\chi_i \equiv |\mathbf{S}_i|/M_i^2 \lesssim 0.8$, with particular emphasis on spins (anti-)aligned with the orbital angular momentum. We note, however, the following explorations outside this "best charted" subset of the parameter

space. Circular binaries with mass ratios up to $q = 1/100$ have been studied in [114, 115]; comparisons for this value of q with fully perturbative calculations have been obtained in the limit of head-on collisions in [116], who report a discrepancy of $\sim 7\%$ in GW energy and momentum, probably in large part due to the discretization error of the numerical simulations. The first direct comparison of numerical results with leading-order self-force prediction was studied in the context of periastron advance in BH binaries in [117]. BH binaries with spins ~ 0.9 have been evolved in [118, 85, 119], but exceeding an apparent barrier of $\chi \approx 0.93$ requires departure from the conformal flatness assumption [120, 61, 86]. The present maximum is $\chi_{1,2} = 0.95$ for aligned spins evolved for 12.5 orbits by Lovelace *et al.* [86]. Finally, we note that emission of GWs efficiently circularizes BH binary orbits [121]. BH binaries are therefore expected to have vanishing eccentricity by the time they enter the frequency window of ground-based detectors, and for this reason most work on GW source modeling has focused on the quasi-circular limit. The derivation of BH momenta, including a small radial component, for quasi-circular initial data in numerical relativity is based either on integrating the PN equations of motion [122, 123] or iterative procedures using several numerical simulations [124, 75, 125, 126]. The decay of eccentricity during the inspiral phase as well as periastron advance has been measured in numerical simulations in [125]. For numerical studies of BH binaries with significant eccentricity as well as arguments why eccentric binaries may represent relevant sources of GWs after all, especially in the more extreme mass ratio regime and for space-based detectors, we refer the reader to [127, 128, 129, 130, 131].

Gravitational waveforms from BH binaries: For illustration, we display in Fig. 1 the real parts of the h_{22} and h_{33} multipoles of the GW strain h obtained for the inspiral and coalescence of a binary of nonspinning BHs with mass ratio $q = 1/4$ [132]. In the course of the inspiral, both amplitude and frequency of the GW signal gradually increase. Close to merger, defined as formation of a common apparent horizon, the GW amplitude reaches a maximum. Eventually it drops exponentially as the merged hole rings down to a stationary Kerr state: see e.g. Fig. 18 in [91].

The qualitative features of the GW signal emitted by different types of binaries can be summarized as follows. (i) The inspiral of two nonspinning, equal-mass BHs is the case most intensively studied by numerical relativity. The wave signal is dominated by the $(l,m) = (2,2)$ multipolar component, which carries $> 98\%$ of the total radiated energy. The
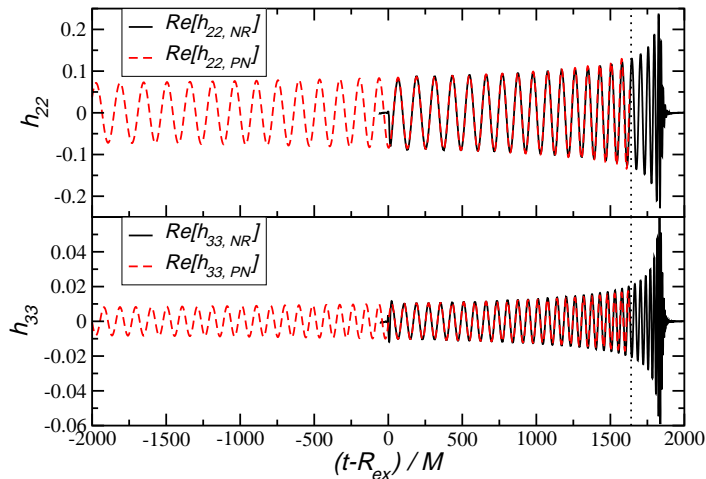
11

Figure 1: Real part of the GW multipoles h_{22} and h_{33} obtained from the inspiral and merger of a nonspinning binary with mass-ratio $q = 1/4$. The dashed red curve represents PN predictions matched to the numerical (solid black) signal. The vertical dotted lines mark the time when the frequency of the $(l, m) = (2, 2)$ multipole has reached $M\omega = 0.1$.

longest numerical simulation by Scheel *et al.* [133] covers 16 orbits and reports a ratio of final to initial BH mass $M_f/M = 0.95162 \pm 0.00002$ and a final spin $S_f/M_f^2 = 0.68646 \pm 0.00004$. (ii) As the mass-ratio decreases, higher-order modes become more prominent [134] and the fractional energy in $(l, m) = (2, 2)$ drops to about 68 % in the limit $q \to 0$ [135]. Motivated by the strong relation of phase and frequency of different (l, m) multipoles, Baker *et al.* [136] view the (l, m) radiation modes as being generated by the corresponding momenta of an *implicit rotating source*; see also [137]. (iii) GW multipoles with odd l are suppressed in the equal-mass limit due to symmetry. (iv) BH binaries with spins aligned with the orbital angular momentum emit stronger GW signals due to an effect sometimes referred to as *orbital hang-up*: equal-mass binaries with $\chi_1 = \chi_2 = 0.757$ radiate about twice as much energy and angular momentum when compared to the nonspinning case [138]. For anti-aligned spins the GW energy decreases by a similar factor. (v) Orbital eccentricity introduces a nonmonotonic behavior of the GW frequency; cf. Fig. 6 in [128]. (vi) Spin-spin and spin-orbit couplings cause a precession of the orbital plane in the case of BH binaries with spins that are not aligned or anti-aligned with the orbital angular momentum. This precession manifests itself in a modulation of the GW amplitude emitted in a fixed angular direction: cf. Fig. 1 in [139].

12

Tests of general relativity: Numerical simulations of binary BH mergers provide an opportunity to study the nonlinearities of the theory and to test the Kerr nature of astrophysical BHs. If GR is the correct theory of gravitation, all BHs in the Universe should be described by the Kerr solution [1], which depends on two parameters: the mass M and the dimensionless spin χ. The remnant of a binary BH merger settles down to the Kerr solution by emitting gravitational radiation at characteristic (complex) quasinormal frequencies $M\omega_{nlm}$ that depend only on χ. Here (l, m) are the usual angular indices, and n is the "overtone number": modes with small n have a longer damping time and should dominate the radiation [140, 45].

The measurement of the real and imaginary part of a single quasinormal mode contains, in principle, enough information to determine the mass and spin of the BH. Together with the accurate determination of the individual BH masses from the inspiral phase this already allows for tests of GR, by testing the GR prediction for mass loss during inspiral and merger and at the same time the strong field dynamics of GR. The measurement of *any* other frequency or damping time then provides a further interesting test of the Kerr nature of the final BH [141]. The feasibility of these tests depends on the characteristics of a given GW detector and on the relative excitation of the modes (see [142, 143] for detailed studies). Quantifying the excitation of quasinormal modes for generic initial data is a formidable technical problem [44, 144], but numerical merger simulations allow sensible estimates of the relative quasinormal mode amplitudes [91, 134]. The relative mode amplitude depends on the binary parameters, and therefore, in principle, the measurement of a multi-mode signal with single or (better) multiple GW detectors can be used to measure the binary mass ratio or the inclination of the final BH spin with respect to the line of sight.

We also remark that the increased signal-to-noise ratio coming from the merger has been shown to *improve* the bounds on alternative theories of gravity that could come from observations of the inspiral only. Keppel and Ajith, for example, discussed this possibility in the context of massive graviton theories, where the graviton mass would modify the dispersion relation of GWs [145]. Formulations of the evolution equations in alternative theories of gravity are in their infancy [146, 147]. This is an interesting line of research, and in the near future we may have more concrete ways to quantify deviations from GR in strong-field mergers.

GW template banks: The key challenge in GW data analysis is to ac-

curately predict and isolate the features of gravitational waveforms in the data stream from GW detectors. This is necessary in order to (i) detect the presence of a GW signal of astrophysical origin, and (ii) determine the parameters of the emitting source. These goals can be achieved by matched filtering, i.e. by cross-correlating the data stream s (composed of detector noise n plus a potential GW signal h) with a bank of theoretical waveform templates h_{λ_i}, where the indices λ_i $(i = 1, \ldots, P)$ denote the P intrinsic and extrinsic source parameters. For this purpose it is imperative to construct a large set of accurate numerical waveforms which cover the relevant parameter space. This task far exceeds the capacity of purely numerical methods. If we assume a seven-dimensional parameter space – one mass ratio and three spin parameters per hole – a mere ten waveforms per parameter would correspond to 10^7 waveforms. Furthermore, using binary waveform models including the long inspiral phase plus merger optimizes the signal-to-noise ratio in GW observations, and the inclusion of merger and ringdown has been shown to provide significant improvements in source localization and distance calculation [148]. Because current numerical simulations cover only about 30 cycles of the inspiral, the generation of complete waveforms requires the combined use of PN and numerical methods. The construction of such GW template banks currently proceeds along either of the following two paths.

(i) The *effective-one-body* (EOB) approach [149, 150] maps the dynamics of the two-body problem in GR into the motion of a particle in an effective metric. The components of the effective metric are currently determined to 3PN order. The EOB method improves upon this model by using additional *pseudo-PN* terms of higher order[1] which are not derived from PN expressions, but calibrated via comparison with numerical results [151, 152, 153, 154, 155]. Further improvements come from using a resummed version of the PN expanded results and from modeling nonadiabatic effects in the inspiral: see e.g. Sec. IV in [156]. The inspiral-plunge waveform resulting from this construction is then matched to a merger-ringdown signal composed of a superposition of quasinormal oscillation modes of a Kerr BH. The total number of free parameters varies between the individual EOB models currently investigated, but in all cases, the general strategy is to calibrate these parameters

---

[1]Comparing an EOB model without such additional calibration against numerical relativity waveforms has been found to result in an accumulated phase difference at merger of 3.6 rad for nonspinning binaries with mass ratios q between 1 and 6 [151].

by comparison with a finite number of numerical simulations.

(ii) *Phenomenological waveform templates* are based on *hybrid waveforms*: the early inspiral is modeled by PN techniques, and the resulting signal is matched (within a specified window) to a numerical waveform describing the last orbits, merger and ringdown. The resulting set of hybrid waveforms are then approximated by a model containing a number of phenomenological parameters which are mapped to the physical parameters of the binaries, such as the mass ratio q. The phenomenological models initially developed for nonspinning binaries in [157, 158, 159], and then extended to the case of spins aligned with the orbital angular momentum [160], are based on hybrid waveforms matched in the *time domain*, whereas the more recent study by Santamaria *et al.* [161] performs the matching in the frequency domain. In spite of such differences in their construction, the final result of all these phenomenological models are closed-form analytic expressions for the waveforms in the frequency domain. An exploration of phenomenological models for equal-mass binaries with spin precession is given in [162].

Both types of template banks are employed in the analysis of GW data. The recent search for GWs from binary BH inspiral, merger and ringdown [163] used phenomenological models for injection, and an EOB model for injection and for the search templates. This search constrained the rate of mergers of binaries with individual masses in the range $[19, 28]$ $M_\odot$ to be no more than 2.0 Mpc^{-3}Myr^{-1} at 90% confidence. Numerical waveforms have also been used inside the GW community-wide *Ninja* project [164] to study the sensitivity of existing GW search algorithms used in the analysis of observational data. For this purpose, numerical relativity waveforms were injected into a simulated data stream designed to mimic ground-based detector noise. The algorithms detected a significant fraction of the injections, but likely require further development, in particular for the purpose of measuring source parameters [165, 166]. A further community wide effort, the *NRAR* project [167], is dedicated to a systematic exploration of the complete BH binary parameter space to develop optimally-calibrated template families to be used in GW data analysis.

One of the most exciting prospects of GW detection is the idea of looking for electromagnetic counterparts to the GW signal. While a *network* of Earth-based detectors is required to localize a GW source by triangulation (see e.g. [168]), a single space-based detectors like LISA may suffice to localize low-redshift sources and determine their luminosity distance. The inclusion of merger and/or of higher multipolar components of the radiation in the

waveform models has been shown to provide significant improvements in source localization and distance determination [169, 148]. For this reason it is very important to construct phenomenological models including higher multipoles of the full inspiral/merger/ringdown waveform. The EOB model has recently been extended in this direction [151].

Accuracy requirements: Clearly, the two approaches for template construction mentioned above require accurate numerical waveforms. Quantifying these accuracy requirements is a nontrivial task. Numerical uncertainties due to finite resolution are directly tested by *convergence analysis*, and the error incurred by extracting GWs at finite radius can be estimated using extrapolation of results from various radii to infinity [170]. The uncertainties in phase and amplitude thus derived, however, depend on the alignment of the waveforms in phase and time; see e.g. Fig. 2 in [132]. Because offsets in phase and time are free parameters in GW data analysis, it is more convenient to measure accuracy and agreement of different waveforms in terms of quantities which take such alignment into account by construction. Such a measure is obtained from the inner product between two waveforms $h(t)$ and $g(t)$ used in the theory of parameter estimation [171, 168]:

$$\langle h, g \rangle \equiv 4\mathbf{Re} \int_0^\infty \frac{\tilde{h}(f)\tilde{g}^*(f)}{S_N(f)} df, \tag{12}$$

where the tilde and asterisk denote Fourier transform and complex conjugate, respectively, and $S_N(f)$ is the one-sided power spectral density of the detector strain noise [172]. In practice, this inner product is to be understood as maximized over constant offsets in time and phase (Δt_0 and $\Delta \phi_0$) between the two waveforms[2]. The signal-to-noise ratio that would be obtained for a physical signal h_e and a model waveform h_m is then given by $\rho_m = \langle h_e|h_m \rangle / ||h_m||$. It is related to the optimal signal-to-noise ratio ρ for a perfect model waveform by the *mismatch* $\mathcal{M}$ [168]:

$$\rho_m = (1 - \mathcal{M})\rho = (1 - \mathcal{M})\langle h_e|h_e \rangle / ||h_e||. \tag{13}$$

To leading order in $||\delta h||$, this definition of the mismatch implies [173, 174]

$$\mathcal{M} = \frac{\langle \delta h|\delta h \rangle - \langle \delta h_{||}|\delta h_{||} \rangle}{2\langle h_e|h_e \rangle} \leq \frac{\langle \delta h|\delta h \rangle}{2\langle h_e|h_e \rangle}, \tag{14}$$

---

[2]For detection of GW events, one often considers the *effectualness* of waveform models (as opposed to *faithfulness*) and in those cases also maximizes the inner product over the source parameters.

16

where $\delta h_{||} = \langle \delta h | h_e \rangle / \langle h_e | h_e \rangle$ is that part of the waveform error parallel to h_e.

Based on these definitions, accuracy requirements are obtained as follows. Two waveforms differing by δh will be indistinguishable for a detector if $\langle \delta h | \delta h \rangle < 1$ [173, 156], such that acceptable waveform models to be used in parameter estimation must lie within a sphere of unit radius of the exact waveform. For the purpose of event detection, we note that the fractional loss in detection of GW signals due to imperfect templates is proportional to the third power of the reduction in the SNR, i.e. $\approx 3\mathcal{M}$. A value of 10% is typically deemed acceptable, corresponding to a mismatch $\mathcal{M} = 3\% \ldots 3.5\%$. For detection efficiency, there arises, however, a complication due to the discrete nature of the template bank. As discussed in detail in Sec. II B of [173], the effective mismatch in a real GW search is given by a contribution due to the actual modeling procedure, plus a term which accounts for the discrete spacing in the parameter space: see their Fig. 3 and Eq. (17). Template banks adopted in LIGO searches use 0.3 for the latter [163, 175] and, in consequence, Lindblom *at al.* [173] recommend a maximum mismatch $\mathcal{M}_{\mathrm{max}} = 0.005$. In terms of the right-hand side of Eq. (14), dubbed *inaccuracy function* in Ref. [156], we summarize the accuracy requirements as (cf. Eq. (10) in Ref. [174])

$$\frac{||\delta h||}{||h||} < \begin{cases} 1/\rho & \text{for parameter estimation,} \\ \sqrt{2\mathcal{M}_{\mathrm{max}}} & \text{for detection.} \end{cases} \tag{15}$$

Accuracy measurements employing the mismatch or $||\delta h||$ have been used to study numerical, semi-analytic and hybrid waveforms. According to the Samurai project [176], relative mismatches of the $l = m = 2$ mode between a variety of purely numerical waveforms for binaries with total mass[3] $M \geq 60 \ M_{\odot}$ are better than 10^{-3}. Hannam *et al.* [177] found errors in the construction of hybrid waveforms to be dominated by PN contributions. Numerical waveforms should be long enough to enable matching at lower frequencies, where PN approximations are more accurate: ~ 3 orbits before merger for the equal-mass, nonspinning case, and ~ 10 orbits for binaries with spins $\chi = 0.5$. MacDonald *et al.* [174] report significantly more demanding requirements of ~ 30 orbits for nonspinning, equal-mass binaries. Similarly, Boyle [178] concludes that longer NR waveforms or more accurate

---

[3]For significantly lower masses, the last 10 orbits and merger signal lie outside the maximum sensitivity range of the current generation of ground-based GW detectors.

PN predictions will be required. The discrepancy largely arises from the use of more stringent accuracy thresholds: $\mathcal{M}_{\max} = 0.005$ in [174] (instead of $\mathcal{M}_{\max} = 0.03$ in [177]) for detection, and $\rho = 40$ for parameter estimation. Most recently, Ohme *et al.* [179] have argued that maximising the match over intrinsic source parameters as well as phase and time shifts may reduce length requirements on numerical waveforms.

A comparison of phenomenological and EOB template banks based on the inaccuracy function has been performed by Damour *et al.* [156]. For advanced ground-based detectors, they conclude that current phenomenological models deviate from the EOB (considered as a target model) beyond acceptable thresholds over a wide range of the parameter space, for both, detection and parameter estimation.

Further reading on BH simulations in the context of GW physics is available in [180, 181, 182, 183].

4. Numerical relativity and astrophysics

Astrophysical observations have provided the strongest evidence to date that BHs exist and play an important role in many physical processes in our Universe. Astrophysical observations of X-ray binaries or quasars, as mentioned in Sec. 1, have a good deal to tell us about BHs. In recent years, numerical relativity simulations of BHs have also deepened our insight into a variety of astrophysical systems. We will first summarize what we have learned from "traditional" electromagnetic observations about the populations of BHs we can expect to exist in the Universe. Then we will discuss some astrophysical implications of numerical relativity.

Expected BH populations: We have already mentioned the two main classes of BHs identified by astrophysical observations. (i) Solar-mass BHs with $M \sim 5 - 20 \ M_\odot$ are usually found in X-ray binaries [184] and are formed as the end-product of the evolution of massive stars. (ii) SMBHs with $M \sim 10^6 - 10^{9.5} \ M_\odot$ are believed to reside in most Active Galactic Nuclei (AGN) [13]. The assembly of these SMBHs is likely to result from a combination of BH mergers and accretion of surrounding matter over cosmological timescales. Evidence for a third class of BHs with $M \sim 10^2 - 10^5 \ M_\odot$ (IMBHs) is tentative at present [185, 186, 187].

GW frequencies are inversely proportional to the system's total mass, and therefore BH masses play a crucial role in binary BH detectability. Earth-based detectors, such as LIGO and Virgo, have an optimal sensitivity band

corresponding to stellar-mass BHs and IMBHs, while the planned space-based detector LISA is most sensitive to high-mass IMBHs and SMBHs. As discussed in the previous section, the expected GW pattern from BH binaries depends on the masses and spins of the binary members. We shall further see below that the gravitational recoil imparted upon the remnants of coalescing binaries strongly depends on spins and mass ratio. So, what do "traditional" electromagnetic observations tell us about BH masses and spins?

Current spin estimates for accreting, stellar mass BHs are usually obtained by modeling the shape of their X-ray spectrum or by analyzing the skew in Fe Kα emission lines. The resulting estimates are all, to some extent, model-dependent, but frequently yield moderate values $\chi \approx 0.1 \ldots 0.8$ and, for some cases, values close to the Kerr limit $\chi = 1$; see e.g. [45, 188] and references therein. Theoretical arguments and observations suggest that stellar-mass BHs in binaries *retain the spin they had at birth*: neither accretion nor angular momentum extraction are likely to change significantly their mass or spin [189, 190]. For SMBHs, spin estimates relying on the shape of the Fe Kα line yield values ranging from moderate $\chi \sim 0.6 \ldots 0.8$ (e.g. [191, 192, 193] to near-critical spins (e.g. [194, 195, 196, 197]). SMBHs are expected to grow by a combination of mergers and accretion. Their spin depends sensitively on the details of these processes and of their growth [198, 199, 200]. SMBH assembly via BH mergers does not appear to be able to account for the large observed spin values; this may indicate that accretion dominates over mergers [201]. In any case, BH spins encode the history of their formation, and it would be extremely useful to have detailed knowledge of the BH spin distribution function. Ultimately, such a detailed census of BH parameters is one of the key targets of future GW observations [202, 203]. For the purpose of numerical modeling of BHs, present measurements indicate that all spin magnitudes ($0 \leq \chi \leq 1$) should be covered.

We have already noted that stellar-mass BHs typically have masses in the range $[5, 20]$ $M_\odot$. Unfortunately, there are no confirmed observations of stellar-mass *binary* BH candidates, so estimates of mass ratios must rely on theoretical models. For stellar-mass binaries, population synthesis codes suggest that q should always be quite close to unity [190]. Measurements of SMBH masses are obtained by observations of stellar motion near galactic centers, as mentioned in Sec. 1, as well as motion of gas discs [204], applications of the virial theorem to the velocity dispersion of stars [14] and reverberation mappings applied to more distant AGNs [205]. An exhaustive list of galaxies with SMBH mass measurements in the range $M \sim 10^5 - 10^9$ $M_\odot$ is

presented by Graham *et al.* [206, 207]. The impact of different SMBH assembly models on the mass and mass ratio distribution of detectable binaries has been discussed by various authors. The general consensus is that mass ratios $q \lesssim 1/10$ (and down to $q \approx 10^{-4}$) should be common [31, 208, 209]. In contrast with the case of stellar-mass BHs, there is by now some observational evidence for SMBH binaries [210, 211, 212, 213, 214]. These observations are not sufficient to tightly constrain SMBH merger rates, but they are at least broadly consistent with merger-tree models predicting tens to hundreds of events during the typical lifetime of a space-based GW detector [215].

A more speculative kind of source for Earth-based detectors consists of the intermediate mass ratio inspiral of a compact object (neutron star or BH) into an IMBH. Another promising source for advanced Earth-based interferometers (albeit with highly uncertain event rates) are IMBH-IMBH mergers. The initial inspiral of these binaries could be detected via space-based interferometers, while the ringdown phase is in the optimal bandwidth for second- and third-generation detectors such as Advanced LIGO and ET, that could therefore be used for "follow-up" ringdown searches [216, 217].

As in the case of BH spins, the observations imply that numerical relativity needs to cover a wide range in q. This can be done most efficiently by bridging the gap between numerical studies and the perturbative modeling of extreme-mass-ratio binaries (e.g. [218, 219, 220]).

From this discussion, it is clear that a detailed knowledge of the spin evolution as well as the generation of gravitational recoil in BH binary mergers is important for understanding the cosmological evolution of SMBHs over cosmological times. We will discuss these effects in turn.

Black-hole spins resulting from mergers: Prior to the 2005 numerical relativity breakthroughs, it was known that "minor mergers" ($q \lesssim 10$) of a large, rotating BH with an isotropic distribution of small objects would tend to spin down the hole [221]. Numerical merger simulations showed that the merger of comparable-mass, nonspinning BHs leads to a final Kerr BH with spin parameter $a/M = 0.69$. The simulations were followed by the development of several models to predict the spin of merger remnants as a function of the binary parameters for generic mass ratios and spins.

The first studies focussed on performing numerical evolutions of the last few orbits of BH binaries, and used the results to calibrate formulae that map the initial binary parameters to values for the spin of the merged hole [97, 134, 118, 222, 223, 224]. It became clear, however, that the binary

inspiral up to the last orbits has the potential to significantly affect the spin distribution (e.g. [225]) and therefore should be included, for example via PN modeling, in the derivation of maps from initial parameters to the merger remnant properties [226, 227, 228, 229, 230]. Predictions for the final spin based on the extrapolation of test-particle calculations to finite mass ratios have been developed in [152, 231], and show remarkably good agreement with numerical results in the comparable-mass regime. A comprehensive review of all spin formulae is beyond the scope of this article, but we refer the reader to the review in [232] and the discussion in Sec. V of [230]. If we assume an ensemble of BH binaries with initially randomly oriented spins, the final spin distribution is peaked around $\chi_f \approx 0.7$ [200, 226, 229]. Campanelli *et al.* [97, 233] reported spin flips by $34 - 103°$ with respect to the initial spin direction of the larger hole; spin flips of this magnitude could provide an explanation for X-shaped radio sources [234]. Kesden *et al.* [230] demonstrated that spin precession over the course of a long inspiral of thousands of orbits tends to align (antialign) the binary BH spins with each other if the spin of the more massive BH is initially partially aligned (antialigned) with the orbital angular momentum, thus increasing (decreasing) the average final spin. Spin precession is stronger for comparable masses, and it could produce significant spin alignment before merger for both SMBHs and stellar-mass BH binaries.

Gravitational recoil: One of the most spectacular results obtained from numerical BH binary simulations is the quantitative prediction of the magnitude of *gravitational recoils* (or *kicks*). In the 1960s it was realized that the emission of linear momentum via GWs must impart a kick on the source due to momentum conservation [235, 236]. In the 1980s, the kick generated in compact binary inspirals and plunges was studied in the framework of PN theory and BH perturbation theory [237, 238, 239]. However, the astrophysical relevance of the gravitational recoil following BH binary mergers remained an open question until the recent numerical relativity breakthroughs.

For the case of an equal-mass, nonspinning BH binary, the net linear momentum emitted in GWs vanishes due to symmetry. Nonzero recoils are therefore only generated in systems where this symmetry is broken through (i) a mass ratio $q < 1$ (equivalently, a symmetric mass-ratio parameter $\eta \equiv q/(1+q)^2 < 1/4$) or (ii) nonvanishing spins.

For zero spins, early numerical studies in the range $q = [1, 1/4]$ found that the kick velocity is well approximated by [57, 240, 241]

$$v_{\text{kick}} = 1.2 \times 10^4 \eta^2 \sqrt{1 - 4\eta}(1 - 0.93\eta) \text{ km/s}. \qquad (16)$$

This result (whose functional form is inspired by Fitchett's analytical work [237]) was confirmed by simulations for smaller mass ratios ($q = 1/10$, [135]) and by analytical work [242]. The maximal recoil obtained from Eq. (16) is $v_{\max} = 175.2 \pm 11$ km/s for $q = 0.36 \pm 0.03$. Small orbital eccentricity $e \leq 0.1$ should introduce corrections proportional to e [243].

Spinning binaries are characterized by seven free parameters (the mass ratio plus three components for each BH spin), and numerical studies inevitably focussed on subsets of the parameter space. It soon became clear that the spin interaction dominates over mass ratio effects. The first studies for equal-mass binaries with spins parallel to the orbital angular momentum revealed kicks of several hundreds km/s, with an extrapolated maximum of ~ 500 km/s for extremal spin magnitudes [244, 245]. Shortly thereafter, the discovery of the so-called *superkicks* marked one of the most surprising outcomes of numerical relativity: binaries for which the spins are perpendicular to the orbital angular momentum and anti-aligned with each other can generate kicks of *thousands* of km/s, with an extrapolated maximum $v_{\max} \sim 4000$ km/s for near-extremal spin magnitudes [233, 246, 247].

Many galaxies harbor SMBHs at their centers, and galaxy mergers should generally lead to the merger of their central BHs [248]. Typical escape velocities range from ~ 10 km/s for dwarf galaxies up to ~ 1000 km/s for giant elliptic galaxies [249]. Large kicks would displace or eject the merged hole from its host, with possibly observable consequences: a softening of the stellar density gradient in the galactic nucleus, off-center radio-loud active galactic nuclei, off-nuclear X-ray sources in nearby galaxies and the generation of electromagnetic signals via interaction of the BH with its gaseous environment [250, 251, 252, 249, 253, 254, 255, 256, 257, 258, 259]. BH ejection represents a potential obstacle for BH growth via merger, and thus puts constraints on merger-history models, which must be able to explain the assembly of SMBHs by redshifts $z \gtrsim 6$ [251, 260, 261]. Observed redshifts of broad-line relative to narrow-line regions in quasar spectra may be interpreted as a smoking gun of BH ejection due to gravitational recoil [262, 214, 263], but alternative interpretations (such as a BH binary, or superposed emission regions from two interacting galaxies) are possible [264, 265, 266, 267].

The interest in astrophysical consequences of large recoils led to numerical studies of the BH parameter space [268, 269, 270, 271, 60, 272, 85, 273, 274, 275]. Phenomenological kick formulas inspired by PN studies [139] and similar to Eq. (16) were proposed to map the input parameters of a given binary configuration to the final kick velocity. Available numerical results

span mass ratios in the range $q \geq 1/10$ and spin magnitudes $|\chi| \leq 0.9$, and are well described by Eq. (2) of Ref. [233] (see also [228, 276]).

The apparent incompatibility between large recoils and the existence of BHs at galactic centers can be resolved by mechanisms that would *align* the individual BH spins with the orbital angular momentum of the binary. One such mechanism are gas torques in the so-called "wet" (gas-rich) mergers, that would produce partial alignment "early on" in the inspiral phase [277]. If partial alignment in gas-rich mergers is the norm, as suggested also by the spin measurements discussed above, PN spin effects will lead to *further* alignment of the spins with the orbital angular momentum, significantly reducing the typical values of recoil velocities [225, 278].

Merger simulations with matter and the Blandford-Znajek effect: Many numerical relativity groups are presently working on binary BH simulations in the presence of matter. Most of this work is trying to understand the signature of electromagnetic counterparts to binary BH mergers: for example, such a signature could be produced by merger events [279] or recoiling BHs [280] "shocking" the surrounding accretion disks. The Georgia Tech group presented the first simulations in full GR of equal-mass, spinning BHs merging in a gas cloud. They found that shocks, accretion and relativistic beaming can produce electromagnetic signatures correlated with GWs, especially when spins are aligned with the orbital axis [281]. Later work by the group focussed on hot, radiatively inefficient accretion flows. In this case, BH binaries exhibit a flare followed by a sudden drop in luminosity associated with the merger, and quasi-periodic oscillations correlated with the GWs during inspiral [282, 283]. The Urbana group simulated equal-mass, nonspinning BH binaries embedded in gas clouds under different assumptions for the motion of the binary with respect to the gas. They found evidence that the accretion rate and luminosity due to bremsstrahlung and synchrotron emission would be enhanced with respect to a single BH of the same mass as the binary, possibly being detectable by LSST [284]. Recent work suggest that the circumbinary disk surrounding BH binaries should not produce detectable electromagnetic counterparts [283, 285]. However, the *magnetic field* produced by the circumbinary disk may extract energy from the orbiting BHs, which ultimately merge within the standard Blandford-Znajek scenario, generating electromagnetic emission along dual or single jets that could be observable to large distance [286, 287, 288, 289].

For further reading, we recommend the following reviews. An excellent

summary of BH mass and spin measurements and (possible) evidence for event horizons based on "traditional" electromagnetic astronomy is given by Narayan [290]. The use of electromagnetic observations of BHs and neutron stars to probe strong-field gravity is reviewed by Psaltis [291]. A more extended summary of numerical results on gravitational recoil can be found in Zlochower *et al.* [275]. For a more general review of numerical BH simulations we recommend Centrella *et al.* [182, 292].

5. Black holes and high energy physics

The breakthroughs in numerical relativity have opened the door to tackle many fundamental problems in BH physics and to address questions of wider interest. A new Golden Era in BH physics is just starting. We summarize below what we think have been the main developments in this relatively short period of time.

Mathematical physics and fundamental issues. A decades-old problem in GR concerns the high-energy collision of two BHs. Due to the dominance of the gravitational interaction at large energies, this process is thought to describe general trans-planckian scattering of particles: at very large center of mass (CM) energies all interactions are "frozen" while gravity is boosted, thus all the details about internal structure of the colliding particles should be washed out. This is further supported by Thorne's hoop conjecture (recently tested in highly dynamical situations [73]), which predicts BH formation from generic high-energy collisions of particles [293]. Because the final BH horizon cloaks all details about the structure of the colliding objects, *matter does not matter* and one can for simplicity study BHs as representing a wide class of colliding objects [38, 39].

For large CM energies, BH collisions are arguably the most violent and nonlinear process one could conceive of. Evolving Einstein's equations in such extreme regimes poses new problems, such as the need to deal with all the different scales involved, and raises several questions. A fundamental issue concerns Cosmic Censorship. In four spacetime dimensions, BHs have

an upper bound on their angular momentum, given by[4]

$$\chi \equiv Sc/(GM^2) \leq 1 \,. \tag{17}$$

Is it possible to tune the impact parameter in such a way as to produce a final object spinning above the Kerr bound, or does nature somehow conspire to always radiate enough angular momentum as to produce a BH? This problem has been addressed in recent years [294, 295, 296, 297].
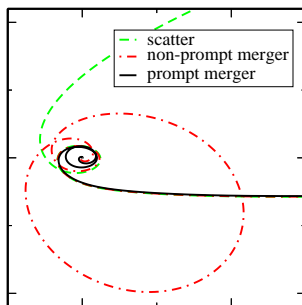

Figure 2: Puncture trajectories of one BH for a scattering orbit ($b[= 3.40M] > b_{\mathrm{scat}}$), a prompt merger ($b[= 3.34M] < b^*$) and a nonprompt merger ($b^* < b[= 3.39M] < b_{\mathrm{scat}}$). Taken from Ref. [295].

We show the trajectory of two equal-mass, nonspinning, colliding BHs in Fig. 2, for CM velocities of around $0.75c$. We notice three distinct regimes. For impact parameters above the *scattering threshold* ($b > b_{\mathrm{scat}}$, the gravitational interaction between the two colliding BHs is relatively weak and they scatter to infinity. For impact parameters below the *threshold of immediate merger* ($b < b_*$), the BHs promptly collide and merge into a single BH. The transition between these two states for $b_* < b < b_{\mathrm{scat}}$ is a nonprompt merger, which puts the BHs in a so-called zoom-whirl orbit, i.e. the number of orbits $n_{\mathrm{orb}} \sim \ln|b - b_*|$. The results show that delayed mergers are necessary in order for the system to radiate excess angular momentum, so that the end product obeys (17). The radiated energy and angular momentum increase strongly as the impact parameter approaches the threshold of immediate merger, as can be seen in Fig. 3. For *head-on* collisions, numerical results suggest that

---

[4]We note that the Earth's spin $\chi_{\mathrm{Earth}} \sim 10^3$, while that of a spinning top $\chi_{\mathrm{top}} \sim 10^{18}$, so (even though the event horizon generators move at the speed of light) BHs rotate "slowly", as measured by their Kerr parameters.
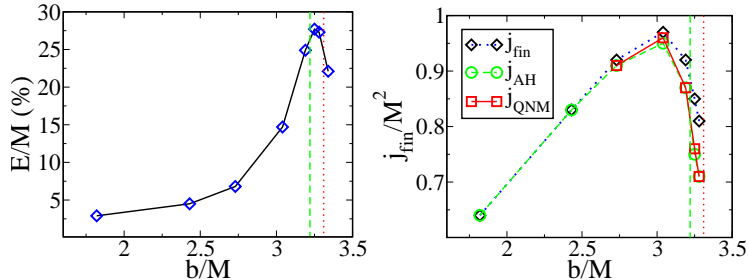
Figure 3: Total energy radiated (left) and final BH spin (right) vs. impact parameter from sequence 2, the latter calculated using several methods. The vertical dashed green (dotted red) line is the estimated threshold of immediate merger b^* (the scattering threshold b_{scat}).

a fraction 14% of the CM energy is radiated in the limit of very large CM energy [294]. For finely tuned impact parameters, the total radiated energy (in GWs) can be of order 30% for a collision with $v \sim 0.75c$ in the CM frame, while the spin of the final hole can reach $\simeq 96\%$ of the bound (17). An open issue is how much CM energy can be radiated for larger boosts. Finally, peak luminosities of around $0.1c^5/G$ are attained in these simulations. This number is orders of magnitude above any electromagnetic phenomena and close to the maximum conjectured possible value [298, 299]. The scattering threshold as a function of boost was studied by Shibata *et al.* and Sperhake *et al.* [295, 296, 297]. For the range of boosts studied it is well approximated by

$$b_{\mathrm{scat}}/M \sim (2.5 \pm 0.05)/v \,. \tag{18}$$

Here M is the total ADM mass and v the velocity of each hole as measured in the CM frame.

Higher-dimensional black holes. Although BH solutions and their properties should in principle fall under the "mathematical physics" category, the activity in this specific field has been so intense that it deserves a subsection of its own. Asymptotically flat higher-dimensional black objects have a much richer structure than their four-dimensional counterparts. For instance, spherical topology is not the only allowed topology for objects with a horizon. One can also have, *e.g.*, black rings, with a donut-like topology. Remarkably, these two different horizon topologies coexist for certain regions in phase-space [300]. Explorations of the stability of general higher-dimensional BHs are in their infancy. Generically it has been conjectured that, for $D \geq 6$, ultra-spinning Myers-Perry BHs will be unstable [301]. This instability has

been confirmed by an analysis of linearized axisymmetric perturbations in $D = 7, 8, 9$ [302]. Clearly, the study of the nonlinear development of these instabilities requires numerical methods, such as the ones reviewed here. A study of this type was very recently presented for nonaxisymmetric perturbations in $D = 5$ [303, 304], where it was found that a single spinning five dimensional Myers-Perry BH is unstable, for sufficiently large rotation parameter (confirming previous conjectures [305, 306, 307]).

General equilibrium states in anti-de Sitter backgrounds only recently started to be explored: nonaxisymmetric solutions have finally been built [308], confirming previous conjectures about their existence [306, 307], and braneworld BHs are now also starting to be explored [309]. Fully dynamical situations are still uncharted territory.

TeV-scale gravity scenarios. The above studies are of direct relevance to some high-energy scenarios. An outstanding problem in high-energy physics is the extremely large ratio between the four dimensional Planck scale, 10^{19} GeV, and the electroweak scale, 10^2 GeV. It has been proposed that this *hierarchy problem* can be resolved by confining the Standard Model to a brane in a higher dimensional space [36, 310, 37, 311].

In such models, the fundamental Planck scale – the energy at which gravitational interactions become strong – could be as low as 1 TeV. Thus, high-energy colliders, such as the Large Hadron Collider (LHC), may directly probe strongly coupled gravitational physics [312, 41, 38, 39]. In fact, such tests may even be routinely available in the collisions of ultra high-energy cosmic rays with the Earth's atmosphere [313, 314, 315], or in astrophysical BH environments [316, 317, 318] (for reviews see [319, 320, 321]). The production of BHs at trans-Planckian collision energies (compared to the fundamental Planck scale) should be well described by using classical GR extended to D dimensions [41, 38, 39, 319, 320, 321]. The challenge is then to use the classical framework to determine the cross section for production and, for each initial setup, the fractions of the collision energy and angular momentum that are lost in the higher-dimensional space by GW emission. This information will be of paramount importance to improve the modelling of microscopic BH production in event generators.

The first models for BH production in parton-parton collisions used a simple black disk approach to estimate the cross section for production [38, 39]. As we already described, only recently exact results for highly relativistic collisions where obtained in four dimensions, using numerical relativity tech-

niques [294, 295, 296, 297]. The extension to higher-dimensional spacetimes is a topic of current investigations [322, 323, 324]. The first numerical results concerning low-energy collisions have been reported last year [324, 325], and some results for high-energy collisions have been presented in [326].

AdS/CFT and holography. In 1997–98, a powerful new technique known as the AdS/CFT correspondence or, more generally, the gauge-gravity duality, was introduced and rapidly developed [33]. This holographic correspondence provides an effective description of a nonperturbative, strongly coupled regime of certain gauge theories in terms of higher-dimensional classical gravity in AdS backgrounds. In particular, equilibrium and nonequilibrium properties of strongly coupled thermal gauge theories are related to the physics of higher-dimensional BHs, black branes and their fluctuations. These studies revealed intriguing connections between the dynamics of BH horizons and hydrodynamics, and offer new perspectives on notoriously difficult problems, such as the BH information loss paradox, the nature of BH singularities and quantum gravity.

Numerical relativity in anti-de Sitter backgrounds is bound to contribute enormously to our understanding of the gauge-gravity duality and is likely to have important applications in the interpretation of observations [35, 327, 328, 329]. For instance, in the context of the gauge-gravity duality, high-energy collisions of BHs have a dual description in terms of *a)* high-energy collisions with balls of deconfined plasma surrounded by a confining phase, and *b)* the rapid localized heating of a deconfined plasma. These are the type of events that may have direct observational consequences for the experiments at Brookhaven's Relativistic Heavy Ion Collider (RHIC) [328, 329]. Numerical relativity in anti-de Sitter is particularly difficult, and so far only very special situations have been handled [330, 331, 332, 333]. Among these, we note the recent numerical proof that pure AdS space is unstable against collapse to BHs [334, 335, 336]

BHs in the context of high-energy physics have also been discussed by Pretorius [180]. A recent review of numerical simulations of black strings in five spacetime dimensions is given by Lehner and Pretorius [337]. Finally we note Kanti's review on BHs at the LHC [321].

6. Conclusions

We conclude this review with a brief summary of the most urgent problems to be tackled by numerical relativity in the three main areas in the near

future.

Gravitational wave physics: In order to meet tight accuracy requirements in GW template generation, especially for parameter estimation, we either need longer numerical waveforms or a denser spacing of templates in the parameter space. Both approaches will require computational resources that grow non-linearly as a function of the accuracy, either because of the slow nature of the inspiral at larger BH separations (see Sec. 2 in [174] for a quantitative discussion) or because of the dimensionality of the parameter space. A second major task is the extension of existing template models to generic binaries with precessing spins and/or smaller mass ratios, bridging the gap to perturbative modeling of extreme mass ratio binaries.

Astrophysics: While existing formulae for the kick and final spin resulting from the coalescence of BHs have been helpful for astrophysical studies, the calibration of generic models as proposed by Boyle *et al.* [338, 339] requires a more comprehensive exploration of the parameter space. The relatively young field of numerical relativity simulations of BHs surrounded by accretion disks will likely improve our insight into expected optical counterparts to BH binary mergers, and thus provide a vital tool for the area of *multi-messanger astrophysics.*

High-energy physics: Arguably the most urgent task is the determination of the scattering cross-section and the loss of energy and momentum in GWs in trans-Planckian scattering of BHs in *arbitrary* dimensions. In view of the stability problems encountered in present studies, it also appears desirable to obtain a better understanding of the well-posedness of the formulations currently employed for such studies. Second, the modeling of BHs in generic spacetimes such as de Sitter and anti-de Sitter is still in its infancy, even if preliminary studies of BHs in non-asymptotically flat spacetimes are encouraging. A better understanding of boundary issues, well-posedness of the formulations and diagnostics such as wave extraction tools and horizon finders will be required to open up this uncharted and fertile ground of research.

References

[1] R. P. Kerr, Phys. Rev. Lett. 11 (1963) 237–238.

[2] R. Giacconi *et al.*, Phys. Rev. Lett. 9 (1963) 439–443.

[3] I. S. Shklovsky, Astrophys. J. 148 (1967) L1–L4.

[4] C. T. Bolton, Nature 235 (1972) 271–273.

[5] B. L. Webster, P. Murdin, Nature 235 (1972) 37–38.

[6] J. van Paradijs, in: American Astronomical Society Meeting Abstracts, Vol. 30 of Bulletin of the American Astronomical Society, 1998, pp. 1291–+.

[7] N. Shaposhnikov, L. Titarchuk, Astrophys. J. 663 (2007) 445–449.

[8] T. A. Matthews, A. R. Sandage, Astrophys. J. 138 (1963) 30.

[9] M. Schmidt, Nature 197 (1963) 1040.

[10] E. E. Salpeter, Astrophys. J. 140 (1964) 796–800.

[11] Y. B. Zel'dovich, I. D. Novikov, Dokl. Akad. Nauk SSSR 155 (1964) 57.

[12] M. J. Rees, Physica Scripta 17 (1978) 193–200.

[13] F. Melia, Supermassive Black Holes, arXiv:0705.1537 [astro-ph].

[14] J. Kormendy, D. Richstone, Ann. Rev. Astron. Astrophys. 33 (1995) 581–624.

[15] D. Richstone *et al.*, Nature 395 (1998) A14–A19.

[16] L. Ferrares, D. Merritt, Astrophys. J. 539 (2000) L9–L12.

[17] K. Gebhardt *et al.*, Astrophys. J. 539 (2000) L13–L19.

[18] R. Schödel *et al.*, Nature 419 (2002) 694.

[19] A. M. Ghez *et al.*, Astrophys. J. 689 (2008) 1044–1062.

[20] LIGO website: http://www.ligo.org.

[21] VIRGO website: https://wwwcascina.virgo.infn.it/.

[22] GEO600 website: http://www.geo600.org/.

[23] ESA-LISA website: http://www.esa.int/esaSC/120376_index_0_m.html.

[24] L. S. Finn, Phys. Rev. D 46 (1992) 5236–5249.

[25] J. Abadie *et al.*, Class. Quantum Grav. 27 (2010) 173001.

[26] K. Belczynski *at al.*, Astrophys. J. 715 (2010) L138–L141.

[27] T. Bulik, K. Belczynski, A. Prestwich, Astrophys. J. 730 (2011) 140.

[28] B. F. Schutz, Classical and Quantum Gravity 28 (2011) 125023.

[29] M. Volonteri, F. Haardt, P. Madau, Astrophys. J. 582 (2003) 559–573.

[30] M. C. Begelman, M. Volonteri, M. J. Rees, MNRAS 370 (2006) 289–298.

[31] A. Sesana, M. Volonteri, F. Haardt, MNRAS 377 (2007) 1711–1716.

[32] K. G. Arun *et al.*, arXiv:0811.1011 [gr-qc].

[33] J. M. Maldacena, Adv. Theor. Math. Phys. 2 (1997) 231.

[34] E. Witten, Adv. Theor. Math. Phys. 2 (1998) 253–291.

[35] D. Mateos, Class. Quantum Grav. 24 (2007) S713–S740.

[36] N. Arkani-Hamed, S. Dimopoulos, G. R. Dvali, Phys. Lett. B429 (1998) 263–272.

[37] L. Randall, R. Sundrum, Phys. Rev. Lett. 83 (1999) 3370–3373.

[38] S. B. Giddings, S. Thomas, Phys. Rev. D 65 (2002) 056010.

[39] S. Dimopoulos, L. G., Phys. Rev. Lett. 87 (2001) 161602.

[40] J. A. Frost *et al*, JHEP 10 (2009) 014.

[41] T. Banks, W. Fischler, hep-th/9906038.

[42] L. Blanchet, Living Reviews in Relativity 9 (4), http://www.livingreviews.org/lrr-2006-4.

[43] S. A. Teukolsky, Astrophys. J. 185 (1973) 635–648.

[44] E. W. Leaver, Phys. Rev. D 34 (1986) 384–408.

[45] E. Berti, V. Cardoso, A. O. Starinets, Class. Quantum Grav. 26 (2009) 163001.

[46] F. Pretorius, Phys. Rev. Lett. 95 (2005) 121101.

[47] M. Campanelli *et al.*, Phys. Rev. Lett. 96 (2006) 111101.

[48] J. G. Baker *et al.*, Phys. Rev. Lett. 96 (2006) 111102.

[49] R. Arnowitt, S. Deser, C. W. Misner, in: L. Witten (Ed.), Gravitation an introduction to current research, John Wiley, New York, 1962, pp. 227–265.

[50] J. W. York, Jr., in: L. Smarr (Ed.), Sources of Gravitational Radiation, Cambridge University Press, Cambridge, 1979, pp. 83–126.

[51] M. Alcubierre, Introduction to 3+1 Numerical Relativity, Oxford University Press, Oxford, 2008.

[52] M. Shibata, T. Nakamura, Phys. Rev. D 52 (1995) 5428–5444.

[53] T. W. Baumgarte, S. L. Shapiro, Phys. Rev. D 59 (1998) 024007.

[54] M. Alcubierre *et al.*, Phys. Rev. D 67 (2003) 084023.

[55] J. G. Baker *et al.*, Phys. Rev. D 73 (2006) 104002.

[56] M. Campanelli *et al.*, Phys. Rev. D 73 (2006) 061501(R).

[57] F. Herrmann *et al.*, Class. Quantum Grav. 24 (2007) S33–S42.

[58] U. Sperhake, Phys. Rev. D 76 (2007) 104015.

[59] B. Brügmann *et al.*, Phys. Rev. D 77 (2008) 024027.

[60] D. Pollney *et al.*, Phys. Rev. D 76 (2007) 124002.

[61] Y. T. Liu, Z. B. Etienne, S. L. Shapiro, Phys. Rev. D 80 (2009) 121503.

[62] J. R. van Meter *et al.*, Phys. Rev. D73 (2006) 124011.

[63] D. Müller, J. Grigsby, B. Brügmann, Phys. Rev. D 82 (2010) 064004.

[64] D. Alic *et al.*, Class. Quantum Grav. 27 (2010) 245023.

[65] Y. Fourés-Bruhat, Acta Math. 88 (1952) 141–225.

[66] Y. Bruhat, in: L. Witten (Ed.), Gravitation: An Introduction to Current Research, Wiley, New York, 1962.

[67] A. E. Fischer, J. E. Marsden, Commun. Math. Phys. 28 (1972) 1–38.

[68] H. Friedrich, Comm. Math. Phys. 100 (1985) 525.

[69] D. Garfinkle, Phys. Rev. D 65 (2002) 044029.

[70] C. Gundlach *et al.*, Class. Quantum Grav. 22 (2005) 3767–3773.

[71] L. Lindblom *et al.*, Class. Quant. Grav. 23 (2006) S447–S462.

[72] L. Lindblom, B. Szilágyi, Phys. Rev. D 80 (2009) 084019.

[73] M. W. Choptuik, F. Pretorius, Phy. Rev. Lett. 104 (2010) 111101.

[74] M. A. Scheel *et al.*, Phys. Rev. D 74 (2006) 104006.

[75] M. Boyle *et al.*, Phys. Rev. D 76 (2007) 124038.

[76] T. Chu *et al.*, Phys. Rev. D 80 (2009) 124051.

[77] M. Boyle *et al.*, Phys. Rev. D 78 (2008) 104020.

[78] G. B. Cook, Living Reviews in Relativity 2000-5, http://www.livingreviews.org/lrr-2000-5.

[79] A. Lichnerowicz, J. Math. Pures et Appl. 23 (1944) 37–63.

[80] J. W. York, Jr., Phys. Rev. Lett. 82 (1999) 1350–1353.

[81] C. W. Misner, Phys. Rev. 118 (1960) 1110.

[82] D. R. Brill, R. W. Lindquist, Phys. Rev. 131 (1963) 471–476.

[83] J. M. Bowen, J. W. York, Jr., Phys. Rev. D 21 (1980) 2047–2056.

[84] S. Brandt, B. Brügmann, Phys. Rev. Lett. 78 (1997) 3606–3609.

[85] S. Dain, C. O. Lousto, Y. Zlochower, Phys. Rev. D 78 (2008) 024039.

[86] G. Lovelace, M. A. Scheel, B. Szilagyi, Phys. Rev. D 83 (2011) 024010.

[87] R. P. Kerr, A. Schild, in: Proceedings of Symposia in Applied Mathematics Vol XVII, 1965, pp. 199–209.

[88] G. B. Cook, H. Pfeiffer, Phys. Rev. D 70 (2004) 104016.

[89] S. Dain, J. L. Jaramillo, B. Krishnan, Phys. Rev. D 71 (2004) 064003.

[90] A. Ashtekar, B. Krishnan, Living Reviews in Relativity 2004-7, http://www.livingreviews.org/lrr-2004-10.

[91] A. Buonanno, G. B. Cook, F. Pretorius, Phys. Rev. D 75 (2007) 124018.

[92] E. Gourgoulhon, gr-qc/0703035.

[93] T. W. Baumgarte *et al.*, Phys. Rev. D 54 (1996) 4849.

[94] P. Anninos *et al.*, Phys. Rev. D 58 (1998) 024003.

[95] J. Thornburg, Class. Quantum Grav. 21 (2004) 743–766.

[96] B. Krishnan, Class. Quantum Grav. 25 (2008) 114005.

[97] M. Campanelli *et al.*, Phys. Rev. D 75 (2007) 064030.

[98] E. T. Newman, R. Penrose, J. Math. Phys. 3 (1962) 566–578.

[99] W. Kinnersley, J. Math. Phys. 10 (1969) 1195–1203.

[100] I. Hinder, B. Wardell, E. Bentivegna, arXiv:1105.0781 [gr-qc].

[101] C. Reisswig *et al.*, Phys. Rev. Lett. 103 (2009) 221101.

[102] C. Reisswig *et al.*, Class. Quantum Grav. 27 (2009) 075014.

[103] M. C. Babiuc *et al.*, arXiv:1011.4223 [gr-qc].

[104] B. Vaishnav *et al.*, Phys. Rev. D 76 (2007) 084020.

[105] Reisswig, C. and Pollney, D., arXiv:1006.1632 [gr-qc].

[106] T. Regge, J. A. Wheeler, Phys. Rev. 108 (1957) 1063–1069.

[107] F. J. Zerilli, J. Math. Phys. 11 (1970) 2203–2208.

[108] F. J. Zerilli, Phys. Rev. Lett. 24 (1970) 737–738.

[109] C. Reisswig *et al.*, Phys. Rev. D 83 (2011) 064008.

[110] T. W. Baumgarte, S. L. Shapiro, Numerical Relativity, Cambridge University Press, 2010.

[111] L. Lehner, Class. Quant. Grav. 18 (2001) R25–R86.

[112] J. L. Jaramillo, J. A. Valiente Kroon, E. Gourgoulhon, arXiv:0712.2332 [gr-qc].

[113] A. Buonanno, Y. Chen, M. Vallisneri, Phys. Rev. D 67 (2003) 024016, [Erratum-ibid. **74**, 029903 (2006)].

[114] C. O. Lousto *et al.*, Phys. Rev. D 82 (2010) 104057.

[115] C. O. Lousto, Y. Zlochower, Phys. Rev. Lett. 106 (2011) 041101.

[116] U. Sperhake *et al.*, arXiv:1105.5391 [gr-qc].

[117] A. Le Tiec *et al.*, arXiv:1106.3278 [gr-qc].

[118] P. Marronetti *et al.*, Phys. Rev. D 77 (2008) 064010.

[119] G. Lovelace *et al.*, Phys. Rev. D 78 084017.

[120] M. D. Hannam *et al.*, Class. Quantum Grav. 24 (2007) S15–S24.

[121] P. C. Peters, J. Mathews, Phys. Rev. 131 (1963) 435–439.

[122] S. Husa *et al.*, Phys. Rev.D 77 (2008) 044037.

[123] B. Walther, B. Brügmann, D. Müller, Phys. Rev. D 79 (2009) 124040.

[124] H. P. Pfeiffer *et al.*, Class. Quantum Grav. 24 (2007) S59–S82.

[125] A. H. Mroue *et al.*, Phys. Rev. D 82 (2010) 124016.

[126] W. Tichy, P. Marronetti, Phys. Rev. D 83 (2011) 024012.

[127] U. Sperhake *et al.*, Phys. Rev. D 78 (2008) 064069.

[128] I. Hinder *et al.*, Phys. Rev. D 82 (2010) 024033.

[129] P. Amaro-Seoane *et al.*, Class. Quant. Grav. 24 (2007) R113–R169.

[130] N. Yunes *et al.*, Phys. Rev. D 80 (2009) 084001.

[131] A. Sesana, Astrophys. J. 719 (2010) 851–864.

[132] U. Sperhake *et al.*, Class. Quantum Grav. 28 (2011) 134004.

[133] M. A. Scheel *et al.*, Phys. Rev. D 79 (2009) 024003.

[134] E. Berti *et al.*, Phys. Rev. D 76 (2007) 064034.

[135] J. A. González, U. Sperhake, B. Brügmann, Phys. Rev. D 79 (2009) 124006.

[136] J. G. Baker *et al.*, Phys. Rev. D 78 (2008) 044046.

[137] B. J. Kelly *at al.*arXiv:1107.1181 [gr-qc].

[138] M. Campanelli, C. O. Lousto, Y. Zlochower, Phys. Rev. D 74 (2006) 041501.

[139] L. E. Kidder, Phys. Rev. D 52 (1995) 821–847.

[140] E. W. Leaver, Proc. Roy. Soc. Lond. A402 (1985) 285–298.

[141] O. Dreyer *et al.*, Class. Quant. Grav. 21 (2004) 787–804.

[142] E. Berti, V. Cardoso, C. M. Will, Phys. Rev. D 73 (2006) 064030.

[143] E. Berti *et al.*, Phys. Rev. D 76 (2007) 104044.

[144] E. Berti, V. Cardoso, Phys. Rev. D 74 (2006) 104020.

[145] D. Keppel, P. Ajith, Phys. Rev. D 82 (2010) 122001.

[146] M. Salgado *et al.*, Phys. Rev. D 77 (2008) 104010.

[147] V. Paschalidis *et al.*, Class. Quant. Grav. 28 (2011) 085006.

[148] S. T. McWilliams *at al.*, arXiv:1104.5650 [gr-qc].

[149] A. Buonanno, T. Damour, Phys. Rev. D 59 (1999) 084006.

[150] A. Buonanno, T. Damour, Phys. Rev. D 62 (2000) 064015.

[151] Y. Pan *et al.*, arXiv:1106.1021 [gr-qc].

[152] A. Buonanno, L. E. Kidder, L. Lehner, Phys. Rev. D 77 (2008) 026004.

[153] T. Damour *et al.*, Phys. Rev. D 77 (2008) 084017.

[154] T. Damour *et al.*, Phys. Rev. D 78 (2008) 044039.

[155] Y. Pan *et al.*, Phys. Rev. D 81 (2010) 084041.

[156] T. Damour, M. Trias, A. Nagar, Phys. Rev. D 83 (2011) 024006.

[157] P. Ajith *et al.*, Class. Quantum Grav. 24 (2007) S689–S700.

[158] P. Ajith *et al.*, Phys. Rev. D 77 (2008) 104017.

[159] P. Ajith, Class. Quant. Grav. 25 (2008) 114033.

[160] P. Ajith *et al.*, arXiv:0909.2867 [gr-qc].

[161] L. Santamaria *et al.*, Phys. Rev. D 82 (2010) 064016.

[162] R. Sturani *et al.*arXiv:1012.5172 [gr-qc].

[163] J. Abadie *at al.*, arXiv:1102.3781 [gr-qc].

[164] Ninja homepage: `https://www.ninja-project.org/doku.php`.

[165] B. Aylott *et al.*, Class. Quantum Grav. 26 (2009) 165008.

[166] B. Aylott *et al.*, Class. Quantum Grav. 26 (2009) 114008.

[167] NRAR homepage: `https://www.ninja-project.org/doku.php?id=nrar:home`.

[168] C. Cutler, E. E. Flanagan, Phys. Rev. D 49 (1994) 2658–2697.

[169] R. N. Lang, S. A. Hughes, N. J. Cornish, arXiv:1101.3591 [gr-qc].

[170] M. Boyle, A. H. Mroué, Phys. Rev. D 80 (2009) 124045.

[171] L. S. Finn, D. F. Chernoff, Phys. Rev. D 47 (1993) 2198–2219.

[172] LIGO Document T0900288-v3:
`https://dcc.ligo.org/cgi-bin/DocDB/ShowDocument?docid=2974`.

[173] L. Lindblom, J. G. Baker, B. J. Owen, Phys. Rev. D 82 (2010) 084020.

[174] I. MacDonald, S. Nissanke, H. P. Pfeiffer, Class. Quantum Grav. 28 (2011) 134002.

[175] B. Abbott *et al.*, Phys. Rev. D 77 (2008) 062002.

[176] M. Hannam *et al.*, Phys. Rev. D 79 (2009) 084025.

[177] M. Hannam *et al.*, Phys. Rev. D 82 (2010) 124008.

[178] M. BoyleArXiv:1103.5088 [gr-qc].

[179] F. Ohme, M. Hannam, S. HusaArXiv:1107.0996 [gr-qc].

[180] F. Pretorius, in: M. Colpi *et al.* (Ed.), Physics of Relativistic Objects in Compact Binaries: From Birth to Coalescence, Springer, New York, 2009.

[181] M. Hannam, I. Hawke, Gen. Rel. Grav. 43 (2011) 465–483.

[182] J. M. Centrella *et al.*, Rev. Mod. Phys. 82 (2010) 3069.

[183] I. Hinder, Class. Quantum Grav. 27 (2010) 114004.

[184] R. A. Remillard, J. E. McClintock, Ann. Rev. Astron. Astrophys. 44 (2006) 49–92.

[185] M. C. Miller, E. J. M. Colbert, Int. J. Mod. Phys. D13 (2004) 1–64.

[186] J. R. Hurley, MNRAS 379 (2007) 93–99.

[187] C. T. Berghea *et al.*, arXiv:0807.1547 [astro-ph].

[188] J. E. McClintock *et al.*, Class. Quant. Grav. 28 (2011) 114009.

[189] A. R. King, U. Kolb, MNRAS 305 (1999) 654–660.

[190] K. Belczynski *et al.*, Astrophys. J. 682 (2008) 474–486.

[191] G. Miniutti *at al.*, arXiv:0905.2891 [astro-ph].

[192] S. Schmoll *et al.*, Astrophys. J. 703 (2009) 2171–2176.

[193] L. C. Gallo *et al.*, arXiv:1009.2987 [astro-ph].

[194] A. C. Fabian *et al.*, MNRAS 361 (2005) 795–802.

[195] L. W. Brenneman, C. S. Reynolds, Astrophys. J. 652 (2006) 1028–1043.

[196] A. Fabian *et al.*, arXiv:0905.4383 [astro-ph].

[197] L. W. Brenneman *et al.*, arXiv:1104.1172 [astro-ph].

[198] C. F. Gammie, S. L. Shapiro, J. C. McKinney, Astrophys. J. 602 (2004) 312–319.

[199] S. A. Hughes, R. D. Blandford, Astrophys. J. 585 (2003) L101–L104.

[200] E. Berti, M. Volonteri, Astrophys. J. 684 (2008) 822.

[201] M. Volonteri, P. Madau, E. Quataert, M. Rees, Astrophys. J. 620 (2005) 69–77.

[202] I. Mandel, V. Kalogera, R. O'ShaughnessyArXiv:1001.2583 [astro-ph].

[203] A. Sesana *et al.*, Phys. Rev. D 83 (2011) 044036.

[204] J. R. Herrnstein *et al.*, Nature 400 (1999) 539–541.

[205] K. Gebhardt *et al.*, Astrophys. J. 543 (2000) L5.

[206] A. W. Graham, PASA 25 (2008) 167–175.

[207] A. W. Graham *at al.*, arXiv:1007.3834 [astro-ph].

[208] S. M. Koushiappas, A. R. Zentner, Astrophys. J. 639 (2006) 7.

[209] L. A. Gergely, B. Mikoczi, Phys. Rev. D 79 (2009) 064023.

[210] S. Komossa, AIP Conf. Proc. 686 (2003) 161–174.

[211] S. Bianchi *et al.*, arXiv:0802.0825 [astro-ph].

[212] M. J. Valtonen *et al.*, Nature 452 (2008) 851–853.

[213] C. Rodriguez *et al.*, Astrophys. J. 697 (2009) 37–44.

[214] F. Civano *et al.*, Astrophys. J. 717 (2010) 209–222.

[215] M. Volonteri, J. M. Miller, M. Dotti, Astrophys. J. 703 (2009) L86–L89.

[216] J. M. Fregeau *et al.*, Astrophys. J. 646 (2006) L135–L138.

[217] P. Amaro-Seoane, L. Santamaria, Astrophys. J. 722 (2010) 1197–1206.

[218] T. Hinderer, E. E. Flanagan, Phys. Rev. D 78 (2008) 064028.

[219] L. Barack, Class.Quant.Grav. 26 (2009) 213001.

[220] E. Poisson, A. Pound, I. Vega, arXiv:1102.0529 [gr-qc].

[221] S. A. Hughes, R. D. Blandford, Astrophys. J. 585 (2003) L101–L104.

[222] L. Rezzolla *et al.*, Astrophys. J. 679 (2008) 1422.

[223] L. Rezzolla *et al.*, Astrophys. J. 674 (2008) L29–L32.

[224] L. Rezzolla *et al.*, Physical Review D 78 (2008) 044002.

[225] J. D. Schnittman, Phys. Rev. D 70 (2004) 124020.

[226] W. Tichy, P. Marronetti, Phys. Rev. D 78 (2008) 081501.

[227] E. Barausse, L. Rezzolla, Astrophys. J. 704 (2009) L40–L44.

[228] C. O. Lousto, M. Campanelli, Y. Zlochower, Class. Quantum Grav. 27 (2010) 114006.

[229] C. O. Lousto *et al.*, Phys. Rev. D 81 (2010) 084023.

[230] M. Kesden, U. Sperhake, E. Berti, Phys. Rev. D 81 (2010) 084054.

[231] M. Kesden, Phys. Rev. D 78 (2008) 084030.

[232] L. Rezzolla, Class. Quant. Grav. 26 (2009) 094023.

[233] M. Campanelli *et al.*, Astrophys. J. 659 (2007) L5–L8.

[234] D. Merritt, R. D. Ekers, Science 297 (2002) 1310–1313.

[235] W. B. Bonnor, M. A. Rotenberg, Proc. R. Soc. Lond. A. 265 (1961) 109–116.

[236] A. Peres, Phys. Rev. 128 (1962) 2471–2475.

[237] M. J. Fitchett, MNRAS 203 (1983) 1049–1062.

[238] M. J. Fitchett, S. Detweiler, MNRAS 211 (1984) 933.

[239] T. Nakamura, M. P. Haugan, Astrophys. J. 269 (1984) 292–296.

[240] J. G. Baker *et al.*, Astrophys. J. 653 (2006) L93–L96.

[241] J. A. González *et al.*, Phys. Rev. Lett. 98 (2007) 091101.

[242] A. Le Tiec, L. Blanchet, C. M. Will, Class. Quantum Grav. 27 (2010) 012001.

[243] C. F. Sopuerta, N. Yunes, P. Laguna, Astrophys. J. 656 (2007) L9–L12.

[244] F. Herrmann *et al.*, Astrophys. J. 661 (2007) 430.

[245] M. Koppitz *et al.*, Phys. Rev. Lett. 99 (2007) 041102.

[246] J. A. González *et al.*, Phys. Rev. Lett. 98 (2007) 231101.

[247] M. Campanelli *et al.*, Phys. Rev. Lett. 98 (2007) 231102.

[248] M. C. Begelman, R. D. Blandford, M. J. Rees, Nature 287 (1980) 307–309.

[249] D. Merritt *et al.*, Astrophys. J. 607 (2004) L9–L12.

[250] M. Boylan-Kolchin, C.-P. Ma, E. Quataert, Astrophys. J. 613 (2004) L37–L40.

[251] Z. Haiman, Astrophys. J. 613 (2004) 36–40.

[252] P. Madau, E. Quataert, Astrophys. J. 606 (2004) L17–L20.

[253] N. I. Libeskind *et al.*, MNRAS 368 (2006) 1381–1391.

[254] A. Loeb, Phys. Rev. Lett. 99 (2007) 041103.

[255] S. Komossa, D. Merritt, Astrophys. J. 689 (2008) L89.

[256] Z. Lippai, Z. Frei, Z. Haiman, Astrophys. J. 676 (2008) L5–L8.

[257] J. Guedes *et al.*, Astrophys. J. 702 (2009) 890.

[258] P. Chang *et al.*, MNRAS 407 (2010) 2007–2016.

[259] J. Guedes *et al.*, Astrophys. J. 729 (2011) 125.

[260] Y. Li *et al.*, Astrophys. J. 665 (2007) 187–208.

[261] M. Volonteri, K. Gültekin, M. Dotti, MNRAS 404 (2010) 2143–2150.

[262] S. Komossa, H. Zhou, H. Lu, Astrophys. J. 678 (2008) L81.

[263] A. Robinson *et al.*, Astrophys. J. 717 (2010) L122–L126.

[264] E. W. Bonning, G. A. Shields, S. Salviander, Astrophys. J. 666 (2007) L13–L16.

[265] T. Bogdanovic, M. Eracleous, S. Sigurdsson, Astrophys. J. 697 (2009) 288–292.

[266] G. A. Shields, E. W. Bonning, S. Salviander, Astrophys. J. 696 (2009) 1367.

[267] M. Vivek *et al.*, MNRAS 400 (2009) L6–L9.

[268] W. Tichy, P. Marronetti, Phys. Rev. D 76 (2007) 061502(R).

[269] J. G. Baker *et al.*, Astrophys. J. 668 (2008) 1140–1144.

[270] B. Brügmann *et al.*, Phys. Rev. D 77 (2008) 124047.

[271] C. O. Lousto, Y. Zlochower, Phys. Rev. D 77 (2008) 044028.

[272] J. G. Baker *et al.*, Astrophys. J. 682 (2008) L29.

[273] C. O. Lousto, Y. Zlochower, Phys. Rev. D 79 (2009) 064018.

[274] C. O. Lousto, Y. Zlochower, Phys. Rev. D 83 (2010) 024003.

[275] Y. Zlochower, M. Campanelli, C. O. Lousto, arXiv:1011.2210 [gr-qc].

[276] J. R. van Meter *et al.*, arXiv:1003.3865 [astro-ph].

[277] T. Bogdanović, C. S. Reynolds, M. C. Miller, Astrophys. J. 661 (2007) L147–L150.

[278] M. Kesden, U. Sperhake, E. Berti, Astrophys. J. 715 (2010) 1006–1011.

[279] M. Megevand *et al.*, Phys. Rev. D 80 (2009) 024012.

[280] M. Anderson *et al.*, Phys. Rev. D 81 (2010) 044004.

[281] T. Bode *et al.*, Astrophys. J. 715 (2010) 1117–1131.

[282] T. Bogdanovic *et al.*, Class. Quant. Grav. 28 (2011) 094020.

[283] T. Bode *et al.*, arXiv:1101.4684 [astro-ph].

[284] B. D. Farris, Y. T. Liu, S. L. Shapiro, Phys. Rev. D 81 (2010) 084008.

[285] P. Mösta *et al.*, Phys. Rev. D 81 (2010) 064017.

[286] C. Palenzuela *et al.*, Phys. Rev. Lett. 103 (2009) 081101.

[287] C. Palenzuela, L. Lehner, S. Yoshida, Phys. Rev. D 81 (2010) 084007.

[288] C. Palenzuela, L. Lehner, S. L. Liebling, Science 329 (2010) 927.

[289] C. Palenzuela *et al.*, Phys. Rev. D 82 (2010) 044045.

[290] R. Narayan, New J. Phys. 7 (2005) 199.

[291] D. Psaltis, arXiv:0806.1531 [astro-ph].

[292] J. M. Centrella *et al.*, Ann. Rev. Nucl. Part. Sci. 60 (2010) 75–100.

[293] K. S. Thorne, in: J. Klauder (Ed.), Magic Without Magic, W.H. Freeman & co, San Francisco, 1972, pp. 231–258.

[294] U. Sperhake *et al.*, Phys. Rev. Lett. 101 (2008) 161101.

[295] U. Sperhake *et al.*, Phys. Rev. Lett. 103 (2009) 131102.

[296] M. Shibata, H. Okawa, T. Yamamoto, Phys. Rev. D 78 (2008) 101501(R).

[297] U. Sperhake *et al.*, Phys. Rev. D 83 (2011) 024037.

[298] K. Thorne, in: T. Deruelle, N. & Piran (Ed.), Gravitational radiation, North-Holland Publishing Company, 1983, pp. 1–57.

[299] G. W. Gibbons, Found.Phys. 32 (2002) 1891–1901.

[300] R. Emparan, H. S. Reall, Living Reviews in Relativity 11 (6), http://www.livingreviews.org/lrr-2008-6.

[301] R. Emparan, R. C. Myers, JHEP 0309 (2003) 025.

[302] O. Dias *et al.*, Phys. Rev. D 80 (2009) 111701.

[303] M. Shibata, H. Yoshino, Phys. Rev. D 81 (2010) 021501.

[304] M. Shibata, H. Yoshino, Phys. Rev. D 81 (2010) 104035.

[305] V. Cardoso, L. Gualtieri, Class.Quant.Grav. 23 (2006) 7151–7198.

[306] V. Cardoso, O. J. Dias, JHEP 0904 (2009) 125.

[307] V. Cardoso *et al.*, JHEP 1001 (2010) 021.

[308] O. J. Dias, G. T. Horowitz, J. E. Santos, arXiv:1105.4167 [hep-th].

[309] P. Figueras, T. Wiseman, arXiv:1105.2558 [hep-th].

[310] I. Antoniadis *et al.*, Phys. Lett. B 436 (1998) 257–263.

[311] L. Randall, R. Sundrum, Phys. Rev. Lett. 83 (1999) 4690–4693.

[312] P. C. Argyres, S. Dimopoulos, J. March-Russell, Phys.Lett. B441 (1998) 96–104.

[313] J. L. Feng, A. D. Shapere, Phys. Rev. Lett. 88 (2002) 021303.

[314] E.-J. Ahn *et al.*, Phys. Rev. D 68 (2003) 043004, hep-ph/0306008.

[315] V. Cardoso *et al.*, Astropart.Phys. 22 (2005) 399–407.

[316] M. Banados, J. Silk, S. M. West, Phys. Rev. Lett. 103 (2009) 111102.

[317] E. Berti *et al.*, Phys. Rev. Lett. 103 (2009) 239001.

[318] T. Jacobson, T. P. Sotiriou, Phys.Rev.Lett. 104 (2010) 021101.

[319] M. Cavaglia, Int.J.Mod.Phys. A18 (2003) 1843–1882.

[320] P. Kanti, Int. J. Mod. Phys. A 19 (2004) 4899–4951.

[321] P. Kanti, Lect.Notes Phys. 769 (2009) 387–423.

[322] H. Yoshino, M. Shibata, Phys. Rev. D 80 (2009) 084025.

[323] M. Zilhão *et al.*, Phys. Rev. D 81 (2010) 084052.

[324] H. Witek *et al.*, Phys. Rev. D 82 (2010) 104014.

[325] H. Witek *et al.*, Phys. Rev. D 83 (2011) 044017.

[326] H. Okawa, K.-i. Nakao, M. Shibata, arXiv:1105.3331 [gr-qc].

[327] S. A. Hartnoll, Class.Quant.Grav. 26 (2009) 224002.

[328] A. J. Amsel, D. Marolf, A. Virmani, JHEP 04 (2008) 025.

[329] S. S. Gubser, S. S. Pufu, A. Yarom, Phys. Rev. D 78 (2008) 066014.

[330] F. Pretorius, M. W. Choptuik, Phys. Rev. D 62 (2000) 124012.

[331] H. Witek *et al.*, Phys. Rev. D 82 (2010) 104037.

[332] P. M. Chesler, L. G. Yaffe, Phys.Rev.Lett. 102 (2009) 211601.

[333] P. M. Chesler, L. G. Yaffe, Phys. Rev. Lett. 106 (2011) 021601.

[334] S. Bhattacharyya, S. Minwalla, JHEP 0909 (2009) 034.

[335] P. Bizon, A. Rostworowski, arXiv:1104.3702 [gr-qc].

[336] D. Garfinkle, L. A. P. Zayas, arXiv:1106.2339 [hep-th].

[337] L. Lehner, F. Pretorius, Final State of Gregory-Laflamme InstabilityarXiv:1106.5184 [gr-qc].

[338] L. Boyle, M. Kesden, S. Nissanke, Phys. Rev. Lett. 100 (2008) 151101.

[339] L. Boyle, M. Kesden, Phys. Rev. D 78 (2008) 024017.